33rd Annual International Conference of the IEEE EMBS
Boston, Massachusetts USA, August 30 - September 3, 2011

Atherosclerotic Plaque Characterization in Optical Coherence Tomography Images

L.S. Athanasiou, T.P. Exarchos *Member, IEEE*, K.K. Naka, L.K. Michalis, F. Prati and D.I. Fotiadis, *Senior Member, IEEE*

***Abstract*— Optical Coherence Tomography (OCT) is a fiber – optic imaging modality which produces high resolution tomographic images of the coronary lumen and outer vessel wall. While OCT images present morphological information in highly resolved detail, the characterization of the various plaque components relies on trained readers. The aim of this study is to extract a set of features in grayscale OCT images and to use them in order to classify the atherosclerotic plaque. Intensity and texture based features we used in order to classify the plaque in four plaque types: Calcium (C), Lipid Pool (LP), Fibrous Tissue (FT) and Mixed Plaque (MP). 50 OCT annotated images from 3 patients were used to train and test the proposed plaque characterization method. Using a Random Forests classifier overall classification accuracy 80.41% is reported.**

I. Introduction

Atherosclerosis [1], [2] is a disease of arteries which is associated with lipid deposition and plaque formation. The various components of atherosclerotic plaques are responsible for different kind of outcomes [3] of the disease. Thus, it is very important to identify and characterize the atherosclerotic plaque components.

Intracoronary Optical Coherence Tomography (OCT) [4], [5] is a new imaging modality which provides high resolution (10 to 15 μm) cross sectional images of the coronary arteries. OCT is rapidly becoming the method of choice in assessing plaque vulnerability [6]. OCT images provide in high resolution, morphological information and experts by examining these images can detect various plaque components. However, manual plaque characterization [7] is rather unreliable due to the lack of well trained OCT readers. Thus a computer - aided method which characterizes the atherosclerotic plaque in OCT images would be of high clinical importance.

In OCT images calcium appears as a low back-scattering heterogeneous region and is fully bordered as it is shown in Fig. 1 (a). Lipid pools are heterogeneous back-scattering plaques [8] and in contrary to caclific regions, lipid pools appear diffusely bordered (Fig. 1 (b)). Fibrous tissue [8] appears as high back-scattering homogeneous areas (Fig. 1 (c)). Finally, mixed plaques appear as heterogeneous back-scattering regions similar to lipid pools and fibrous tissue (Fig. 1 (c)).

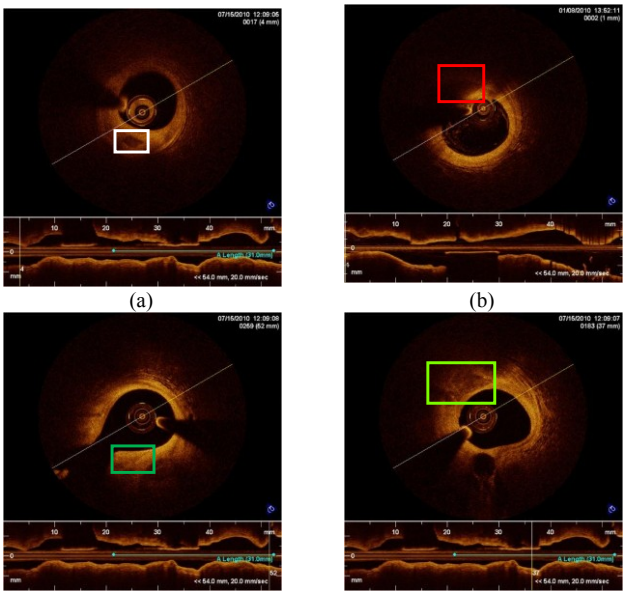

Fig. 1: Plaque appearance in OCT images. (a) Lipid pool appearance, (b) Calcium appearance, (c) Fibrous tissue appearance, (d) Mixed plaque appearance.

Xu *et al.* [9] used histological examinations and correlated the backscattering (μ_b) and attenuation (μ_t) coefficients with calcium (C), lipid pool (LP) and fibrous tissue (FT). In a similar attempt, van Soest *et al.* [10] correlated the attenuation (μ_t) coefficient with healthy vessel wall, intimal thickening, lipid pool (LP) and macrophage infiltration.

In this paper a plaque characterization method based on grayscale OCT images is proposed. The method can be described in two steps:

i. A set of intensity [11] and texture based features [12], [13] is extracted from the pixels that belong to the plaque regions.
ii. Each pixel is classified to one of the four plaque types: calcium (C), lipid pool (LP), fibrous tissue (FT) and mixed plaque (MP).

Currently, a plaque characterization method that uses only grayscale OCT images and classifies the plaque to four plaque types: C, LP, FT and MP, is presented for the first

L.S. Athanasiou, and D.I. Fotiadis are with the Unit of Medical Technology and Intelligent Information Systems, Dept of Materials Science and Engineering, University of Ioannina, GR 45110 (email: lmathanas@cc.uoi.gr, corresponding author phone: +302651008803; fax: +302651008889; e-mail: fotiadis@cs.uoi.gr).

T.P. Exarchos is researcher in Biomedical Research Institute – FORTH, GR 45110 Ioannina, Greece (email: exarchos@cc.uoi.gr)

K.K. Naka and L.K. Michalis are with the Michaelideion Cardiac Center, Dept. of Cardiology in Medical School, University of Ioannina, GR 45110 Ioannina, Greece (email: anaka@cc.uoi.gr, lmihalis@cc.uoi.gr).

F. Prati is with the Interventional Cardiology, San Giovanni Hospital, Via dell'Amba Aradam, 8, 00184 Rome, Italy (email: fprati@hsangiovanni.roma.it)

time. Using the Random Forests classifier the methods overall classification accuracy is 80.41%.

II. Materials And Methods

A. Feature extraction

For each pixel of the plaque regions, for a 11×11 neighborhood, a set of features is extracted. The feature set includes texture and intensity based features. The texture features which are calculated in the proposed method are the Co-occurrence Matrices [13] and the Local Binary Patterns (LBP) [12]. The entropy and the mean value [11] of the neighborhood are the intensity features that are calculated. The texture and intensity features are described bellow in detail.

Co-occurrence Matrix

The Co-occurrence Matrix is computed over all the pixels of an image I. For a pixel of an image I with coordinates i, j, the co-occurrence value is defined as the distribution of co-occurrence values at a given distance (D_x, D_y) from this pixel. For an image $I(i,j): 1 \le i \le k,\ 1 \le j \le l$, with dimensions $k \times l$, the co-occurrence matrix $C_M = C_{(D_x,D_y)}(i,j)$ is defined as:

$$C_M = \sum_{n=1}^{k}\sum_{m=1}^{l}\begin{cases}1, & if\ I(n,m)=i\ and\ I(n+D_x,m+D_y)=j\\ 0, & otherwise\end{cases}, \quad (1)$$

where (D_x, D_y) are defined as:

$$D_x = D\cdot cos(\theta),\ D_y = D\cdot sin(\theta), \quad (2)$$

$\theta = [0^0, 45^0, 90^0, 135^0]$ and D is the distance between the pixels. In our experiments we tested various distance values ($D = \{2,3,5\}$) and we chose $D=2$ to reduce the computational time for the computation of the co-occurrence matrix. The dimension of the co-occurrence matrix is $L \times L$, where L is the number of gray-levels of the image I. From the co-occurrence matrix $C_M = C_{(D_x,D_Y)}(i,j)$ for each angle $\theta = [0^0, 45^0, 90^0, 135^0]$ we compute the following measures [11]:

Contrast:

$$f^{\theta}_{contrast} = \sum_{i=1}^{L}\sum_{j=1}^{L}(i-j)^2 C_M\ . \quad (3)$$

Correlation:

$$f^{\theta}_{correlation} = \sum_{i=1}^{L}\sum_{j=1}^{L}C_M\left[\frac{(i-\mu_i)(j-\mu_j)}{\sqrt{(\sigma_i)^2(\sigma_j)^2}}\right], \quad (4)$$

where:

$$\mu_i = \sum_{i=1}^{L}\sum_{j=1}^{L} iC_M,\ \mu_j = \sum_{i=1}^{L}\sum_{j=1}^{L} jC_M,\ \sigma_t^2 = \sum_{j=1}^{L}\sum_{i=1}^{L} C_M(i-\mu_i^2), \quad (5)$$

and $\sigma_j^2 = \sum_{j=1}^{L}\sum_{i=1}^{L} C_M(j-\mu_j^2)$.

Energy:

$$f^{\theta}_{energy} = \sum_{i=1}^{L}\sum_{j=1}^{L} {C_M}^2\ . \quad (6)$$

Homogeneity:

$$f^{\theta}_{homogeneity} = \sum_{i=1}^{L}\sum_{j=1}^{L}\frac{C_M}{1+|i-j|}\ . \quad (7)$$

Thus, from the co-occurrence matrix 16 features can be computed; four features for each angle $\theta = [0^0, 45^0, 90^0, 135^0]$.

Local Binary Patterns

Local Binary Patterns [12], [14] (LBP) can determine uniform texture patterns into circular neighborhoods. Local Binary Patterns are based on a circular symmetric neighborhood of P members of a circle with radius R. We used a well known LBP the uniform rotation LBP, $LBP^{riu2}_{P,R}$ [15] which is defined as:

$$LBP^{riu2}_{P.R} = \begin{cases}\sum_{p=0}^{P-1} s(g_p - g_c), & if\ U(LBP_{P,R}) \le 2\\ P+1, & otherwise\end{cases}, \quad (8)$$

where g_c is the intensity of the center pixel, g_p are the intensities of the circularly symmetric neighborhood and $U(LBP_{P,R})$ is defined as:

$$U(LBP_{P,R}) = |s(g_{P-1}-g_c) - s(g_0-g_c)| + \sum_{p=1}^{P-1}|s(g_p-g_c) - s(g_{p-1}-g_c)|, \quad (9)$$

and the function $s(x)$ is defined as: $s(x) = \begin{cases}1, & x \ge 0\\ 0, & x < 0\end{cases}$. The output of the $LBP^{riu2}_{P,R}$ is a set of discrete values from 0, 1, 2, ..., $P+1$. In order to compute the uniform rotation LBP we use radius $R=1$ and $P=8$ members.

Entropy

The entropy [11] E_I of an image I is defined as:

$$E_I = \sum_{i=0}^{L-1} p_i\, log_2\left(\frac{1}{p_i}\right) \quad (10)$$

where: $p_i = \frac{\#\ pixels\ with\ intensity\ i}{total\ \#\ of\ pixels}, 0 \le i \le L-1.$

Mean value

The mean value [11] M of a pixel (i,j) is defined, over a neighborhood of the pixel (i,j), as:

$$f_{mean} = \frac{1}{K}\sum_{(o,q)\in N} I(o,q) \quad (11)$$

where: K is the number of pixels in the N neighborhood

and (o,q) are the positions of the pixels neighborhood N.

B. Classification

Random Forests [16] is an ensemble classifier. It consists of many tree structured classifiers. Each tree of the forest cast a unit vote for the most popular class at input x. The predicted class is the one that most of the decision trees "vote". For the construction of the tree a subset of instances is randomly selected from the dataset. Only a subset f of the total set of features F is employed as the candidate splitters of the node of the tree. The number of the selected features is held constant during the forest growing. The number of the selected features plays an important role on the performance of the random forests algorithm since reducing f reduces both the correlation and the strength and increasing it increases both. However, the choice of the value of f is usually made either by a greedy search that tests every possible value to choose the optimal one, either by choosing *a priori* one of the values commonly used in the literature. These values are: $\frac{1}{2}sqrt(F)$, $sqrt(F)$, $2sqrt(F)$, $log_2(F)$.

III. Dataset

To be able to train and test the proposed plaque characterization method we used 50 OCT images from 3 patients. An expert annotated these 50 frames as containing: C, LP, FT and MP. The data were provided by the San Giovanni Hospital of Rome. The images were acquired using a Frequency Domain (FD - OCT) OCT equipment (LightLab Imaging, Inc).

In these 50 frames, 46 frames were used to train and test the proposed method and the rest 4 were used as application examples. From the 45 OCT images: 8 regions were annotated as containing C, 35 as containing LP, 3 as containing FT and 3 as containing MP. In order to create a balanced dataset ($SET_{Ballanced}$), 1400 pixels were randomly selected from each one of the: C, LP, FT and MP plaque regions.

IV. Results

A. Classification results

We performed 10 – fold cross validation for the balanced dataset ($SET_{Ballanced}$). Several numbers of trees and features were tested in order to find the best parameters of the Random Forests classifier. The best results are obtained using 140 trees and 10 features; an overall accuracy of 80.41% is achieved as it is shown in Table I. Additionally the confusion matrix when applying 10-fold cross validation method on the $SET_{Ballanced}$ it is shown in Table II.

TABLE I: Accuracy of the RF classifier using different number of trees and features.

Accuracy (%)					
	#features				
#trees	**6**	**8**	**10**	**12**	**14**
100	80.02	80.11	80.21	79.96	80.02
120	80.2	80.18	80.11	79.82	79.93
140	80.21	80.25	**80.41**	79.93	79.95
160	80.11	80.11	80.32	79.98	80.07
180	80.29	80.29	80.40	80.05	80.04

B. Application examples

The results of the proposed method applied on four different OCT frames, are shown in Fig 2.

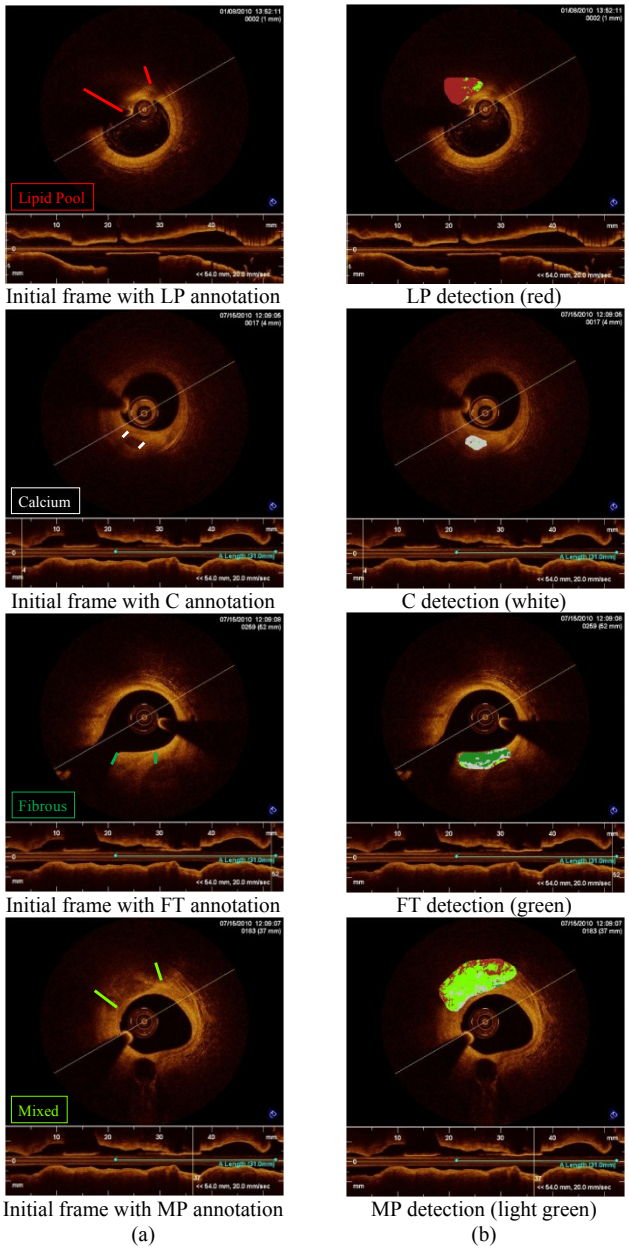

Fig. 1: The results of the proposed plaque characterization method through an application example applied to four OCT frames. (a) The initial frames with the expert's annotations, (b) The results of the proposed method over the initial frames. LP (red): lipid pool, C (white): calcium, FT (green): fibrous tissue, MP (light green): mixed plaque.

TABLE II: THE CONFUSION MATRIX WHEN APPLYING 10-FOLD CROSS VALIDATION METHOD ON THE $SET_{Ballanced}$ USING RANDOM FORESTS CLASSIFIER (140 TREES AND 10 FEATURES).

Confusion Matrix

	C	LP	FT	MP	Total
C	**1153**	52	71	124	**1400**
LP	127	**1081**	17	175	**1400**
FT	59	8	**1302**	31	**1400**
MP	175	195	63	**967**	**1400**

V. DISCUSSION

In this work, a plaque characterization method, for OCT images, based on texture and intensity features is presented. The method extracts a set of features and characterizes the different atherosclerotic plaque formations. Using only the OCT grayscale images the plaque is classified to four plaque components namely: C, LP, FT and MP. A Random Forests classifier is employed and the overall classification accuracy is 80.41 %. Additionally the classification accuracy of C, LP, FT and MP plaque types is 82.35%, 77.21%, 93% and 69.07%, respectively.

The methods described in the literature [9], [10] attempted to correlate the backscattering (μ_b) and attenuation (μ_t) coefficients with various plaque formations. Both methods analyze the optical signal of the OCT equipment. One of the main difficulties of these methods is the distinction between LP and C plaque types [10].

Currently a different approach is presented that addresses the above limitation. The method uses for the first time only the grayscale OCT images in order to characterize the atherosclerotic plaque. The plaque is characterized to four plaque types instead of three [9], [10]. In addition, the classification accuracy of the method in classifying LP and C plaque types is 77.21% and 82.35%, respectively.

Since manual plaque characterization is rather unreliable due to the lack of well trained OCT readers, the proposed plaque characterization method can be used for clinical purposes. In addition, the accurate detection of the C plaque (82.35%) enhances the clinical value of the proposed method since C is a plaque type with high clinical interest [17], [18].

VI. CONCLUSIONS

Atherosclerotic plaque characterization is crucial for early diagnosis and treatment of Coronary Artery Disease (CAD). We presented a computer aided method for characterizing the atherosclerotic plaque in OCT images. The method is based on OCT grayscale images and an overall accuracy 80.41% is achieved. Further improvements will focus on the employment of additional features, in order to enhance the accuracy of the proposed method and of a border detection algorithm, in order to present a fully automated plaque characterization method.

REFERENCES

[1] E. Falk, "Pathogenesis of atherosclerosis," *Journal of the American College of Cardiology,* vol. 47, pp. C7-12, Apr 2006.

[2] P. C. Choy, Y. L. Siow, D. Mymin, and K. O, "Lipids and atherosclerosis," *Biochemistry and Cell Biology-Biochimie Et Biologie Cellulaire,* vol. 82, pp. 212-224, Feb 2004.

[3] G. K. Hansson, "Inflammation, atherosclerosis, and coronary artery disease," *N Engl J Med,* vol. 352, pp. 1685-1695, Apr 2005.

[4] D. Huang, E. A. Swanson, C. P. Lin, J. S. Schuman, W. G. Stinson, W. Chang, M. R. Hee, T. Flotte, K. Gregory, C. A. Puliafito, and et al., "Optical coherence tomography," *Science,* vol. 254, pp. 1178-1181, Nov 1991.

[5] E. Regar, F. Prati, and P. W. Serruys, *Intracoronary OCT application: methodological considerations*. Abingdon: Taylor & Francis, 2006.

[6] F. Prati, E. Regar, G. S. Mintz, E. Arbustini, C. Di Mario, I. K. Jang, T. Akasaka, M. Costa, G. Guagliumi, E. Grube, Y. Ozaki, F. Pinto, P. W. J. Serruys, and E. s. O. R. Document, "Expert review document on methodology, terminology, and clinical applications of optical coherence tomography: physical principles, methodology of image acquisition, and clinical application for assessment of coronary arteries and atherosclerosis," *European Heart Journal,* vol. 31, pp. 401-415, Feb 2010.

[7] K. Jang, G. J. Tearney, B. MacNeill, M. Takano, F. Moselewski, N Iftima, M Shishkov; S. Houser, H. T. Aretz, E. F. Halpern, and B. E. Bouma, "In Vivo Characterization of Coronary Atherosclerotic Plaque by Use of Optical Coherence Tomography," *Circulation*, vol.111, pp. 1551-1555, Mar 2005.

[8] H. Yabushita, B. E. Bouma, S. L. Houser, H. T. Aretz, I. K. Jang, K. H. Schlendorf, C. R. Kauffman, M. Shishkov, D. H. Kang, E. F. Halpern, and G. J. Tearney, "Characterization of human atherosclerosis by optical coherence tomography," *Circulation,* vol. 106, pp. 1640-1645, Sep 2002.

[9] C. Y. Xu, J. M. Schmitt, S. G. Carlier, and R. Virmani, "Characterization of atherosclerosis plaques by measuring both backscattering and attenuation coefficients in optical coherence tomography," *Journal of Biomedical Optics,* vol. 13, pp.13-3, May-Jun 2008.

[10] G. van Soest, T. Goderie, E. Regar, S. Koljenovic, G. L. J. H. van Leenders, N. Gonzalo, S. van Noorden, T. Okamura, B. E. Bouma, G. J. Tearney, J. W. Oosterhuis, P. W. Serruys, and A. F. W. van der Steen, "Atherosclerotic tissue characterization in vivo by optical coherence tomography attenuation imaging," *Journal of Biomedical Optics,* vol. 15, pp. 15-1, Jan-Feb 2010.

[11] R. C. Gonzalez and R. E. Woods, *Digital image processing*, 2nd ed. Upper Saddle River, N.J.: Prentice Hall, 2002.

[12] L. Nanni, A. Lumini, and S. Brahnam, "Local binary patterns variants as texture descriptors for medical image analysis," *Artif Intell Med,* vol. 49, pp. 117-125, Jun 2010.

[13] M. Tuceryan and A. K. Jain, *Texture Analysis - The handbook of Pattern Recognition and Computer Vision*. Sigapore: World Scientific, 1998.

[14] M. Pietainen, "Image analysis with local binary patterns," *Image Analysis, Proceedings,* vol. 3540, pp. 115-118, 2005.

[15] T. Ojala, M. Pietikainen, and T. Maenpaa, "Multiresolution gray-scale and rotation invariant texture classification with local binary patterns," *Ieee Transactions on Pattern Analysis and Machine Intelligence,* vol. 24, pp. 971-987, Jul 2002.

[16] L. Breiman, "Random forests," *Machine Learning,* vol. 45, pp. 5-32, Oct 2001.

[17] C. von Birgelen, G. S. Mintz, D. Bose, D. Baumgart, M. Haude, H. Wieneke, T. Neumann, J. Brinkhoff, M. Jasper, and R. Erbel, "Impact of moderate lesion calcium on mechanisms of coronary stenting as assessed with threem dimensional intravascular ultrasound in vivo," *American Journal of Cardiology,* vol. 92, pp. 5-10, Jul 2003.

[18] R. Virmani, A. P. Burke, F. D. Kolodgie, and A. Farb, "Vulnerable plaque: the pathology of unstable coronary lesions," *J Interv Cardiol,* vol. 15, pp. 439-446, Dec 2002.